Available online at www.sciencedirect.com
SCIENCE DIRECT®
Physics of the Earth and Planetary Interiors 141 (2004) 243–252
PHYSICS OF THE EARTH AND PLANETARY INTERIORS
www.elsevier.com/locate/pepi

Influence of the zone of weakness on dip angle and shear heating of subducted slabs

Martin Kukačka*, Ctirad Matyska

Department of Geophysics, Faculty of Mathematics and Physics, Charles University, V Holešovičkách 2, 180 00 Praha 8, Czech Republic

Accepted 24 November 2003

Abstract

We study the importance of the zones of weakness and the pattern of downgoing flow in steady-state models of subducting lithosphere, which interacts mechanically and thermally with the ambient mantle. The non-linear system of governing equations consists of (i) the momentum equation in stream function formulation and (ii) the steady-state heat transfer equation including conduction and advection of heat and dissipation. A finite element method has been applied to this system. We consider the viscosity to be a non-linear function of both the temperature and the stream function. In steady-state two-dimensional (2D) flow, the stream function isolines follow material trajectories. They are used to follow the top of the subducting slab, which because of its possible increase in water content, is assumed to have a lower viscosity. The zone of weakness has been thus obtained in the self-consistent fashion since the stream function as well as the temperature are the output from our modeling and no a priori assumptions about the shape of the bending lithosphere are taken into account. It was shown that several orders decrease of viscosity in the zone of weakness is required to obtain the dip angle of about 45°. If the decrease of viscosity is not sufficient enough, the subducted slab either sinks almost vertically or does not exhibit a plate-like behavior. We have also demonstrated that shear heating can unrealistically increase at the zone of weakness for fast subductions if decrease of viscosity is underestimated.

Keywords: Subduction; Numerical modeling; Zone of weakness; Shear heating; Dip angle

1. Introduction

The paradigm of plate tectonics requires simultaneous existence of both the relatively rigid plates and the zones of weakness, which enable subduction of plates representing main plate-driving forces (Lithgow-Bertelloni and Richards, 1998) and which are necessary for generation of toroidal plate motions (e.g. Ribe, 1992; Bercovici, 2003). Geodynamic numerical modeling demonstrated that various rheological effects can form shear zones, e.g. self-lubricating rheology (Bercovici, 1995, 1996, 2003), Bingham-type rheology or incorporation of the yield stress (Tackley, 2000a,b), the existence of which stems from the laboratory experiments (Kohlstedt et al., 1995).

On the other hand, the nucleation and the maintenance of the zones of weakness is very complicated because a series of mechanisms can play a role in this problem (Doin and Henry, 2001); see also the review by Regenauer-Lieb and Yuen (2002). In the kinematic models, where the velocity field is prescribed a

* Corresponding author.
E-mail addresses: martin.kukacka@mff.cuni.cz (M. Kukačka), ctirad.matyska@mff.cuni.cz (C. Matyska).

0031-9201/$ – see front matter © 2004 Elsevier B.V. All rights reserved.
doi:10.1016/j.pepi.2003.11.004

priori and the equation of heat transfer is solved to obtain temperature distribution, which plays a key role in mineralogical considerations (e.g. Peacock, 2000; Bina et al., 2001), this problem is avoided since the equations describing mechanical (dynamic) part of subduction are not solved. In many dynamic models, where subducting plate is evolved in the framework of time-dependent thermal convection, the zone of weakness is defined in the form of an a priori prescribed fault (e.g. Billen and Gurnis, 2001; van Hunen, 2001; Čížková et al., 2002).

The aim of our study is to consider the system, where the Stokes problem determining the velocity of motion and the steady-state heat transfer equation are taken into account simultaneously, and to deal with the self-consistent generation of the zone of weakness by means of lubrication due to both the water (Billen and Gurnis, 2001; Karato, 2002; Ono et al., 2002; Regenauer-Lieb and Yuen, 2002) and the thermo-mechanical feedback from the temperature dependence of viscosity (e.g. Karato and Wu, 1993). Such a lubricated system exhibits different behaviour from the non-lubricated one (Lenardic and Kaula, 1994). Seeking the solution of the steady-state system, which is strongly non-linear, requires to overcome some numerical difficulties by introducing a special mathematical approach. On the other hand, the advantage of such a formulation is that we deal with the mature subduction only without any transition time-dependent states.

Although steady-state solutions of time-dependent mantle convection, in which subduction processes play an important role, need not be stable under the Earth's condition, they are able to exhibit various aspects of the subduction, e.g. stress–strain state of the lithosphere and, consequently, also the geometry of the subducting slab. This is the reason why we think that studies of steady-state systems are able to yield an insight into the basic physics of subduction.

2. Basic equations

The mantle and the lithosphere were described as a viscous fluid in the first models of subducting lithosphere (e.g. Bird, 1978; Vilotte et al., 1982) in 1980s. Although current numerical models deal with visco-plastic or even more complicated types of rheology, pure viscous models (Billen and Gurnis, 2001) are still in use. The basic equations governing the thermal convection in a viscous fluid come from the laws of conservation of mass, momentum and energy. There are two simplifications widely used in the modeling of the mantle convection: the inertial forces are neglected and the mantle is considered to be an incompressible fluid. In this case the mantle convection is governed by the continuity equation in the form

$$\nabla \cdot \boldsymbol{v} = 0, \tag{1}$$

and by the momentum equation

$$-\nabla p + \nabla \cdot (\eta(\nabla \boldsymbol{v} + (\nabla \boldsymbol{v})^{\mathrm{T}})) + \boldsymbol{f} = 0, \tag{2}$$

where p denotes the non-hydrostatic pressure, η the dynamic viscosity, $\boldsymbol{v}$ the velocity and $\boldsymbol{f}$ represents body forces. The symbol $\cdot$ denotes the scalar product and the superscript $^{\mathrm{T}}$ denotes transposition. These equations together with appropriate boundary conditions are known as the Stokes problem. The heat transfer equation must be added to complete the system of equations because the body force $\boldsymbol{f}$ is the buoyancy force generated by thermal anomalies and the viscosity η is strongly dependent on temperature. In this paper, we will study the state of mature subduction and thus we will take into account only the steady-state heat transfer equation:

$$\rho c_p \boldsymbol{v} \cdot \nabla T = \nabla(k \nabla T) + \boldsymbol{D} : \nabla \boldsymbol{v}, \tag{3}$$

where ρ is the density, c_p the heat capacity, T the temperature, k the thermal conductivity, and $\boldsymbol{D} = \eta(\nabla \boldsymbol{v} + (\nabla \boldsymbol{v})^{\mathrm{T}})$ is the deviatoric part of the stress tensor and : represents the total scalar product of tensors.

The rheological behaviour of some mineralogical system in the lithosphere have been investigated experimentally and the brittle–ductile–creep model has been proposed (Kohlstedt et al., 1995; Watts, 2001). The topmost part of the lithosphere is brittle and its strength increases with increasing pressure. Underlying thicker layer is ductile and its strength is almost independent on the pressure. Below these two layers, in which rock behaves like an elasto-plastic solid, creep mechanisms dominate.

The creep properties of dry rocks and minerals are described by the power-law creep equation in the form:

$$\dot{e} = A \sigma^n d^{-m} \exp\left(-\frac{Q + pV}{RT}\right), \tag{4}$$

where $\dot{e} = \sqrt{\dot{\boldsymbol{e}} : \dot{\boldsymbol{e}}}$, $\dot{\boldsymbol{e}} = (\nabla \boldsymbol{v} + (\nabla \boldsymbol{v})^{\mathrm{T}})/2$, is the strain rate, $\sigma = \sqrt{\boldsymbol{D} : \boldsymbol{D}}$, A the material constant, d the grain size, Q the activation energy, V the activation volume and R denotes the gas constant (e.g. Karato and Wu, 1993). This formula incorporates two steady-state creep mechanisms: the diffusion creep characterized by $n = 1$ and $m = 3$ observed at low stresses and the dislocation creep characterized by $n = 3$ and $m = 0$, which appears at higher stresses.

We use Euler framework and thus we neglect the uppermost elasto-plastic layers and consider only creep properties. However, purely viscous lithosphere would be too stiff at shallow part because of its temperature-dependence. In order to overcome this obstacle, we introduce yielding viscosity $\eta_{\max}$ (see Eq. (8)). Although the used creep rheology is a simplification of the the lithospheric rheological behaviour, the magnitude of the viscosity is in a reasonable range.

3. The model setup

The governing equations of mantle convection (1)–(3) are solved in a rectangle domain Ω, see Fig. 1. To be able to study the flow pattern at the contact of the subducting and the overriding plates, we set the dimensions of the rectangle to 300×100 km. Since the model is shallow, the buoyant forces are neglected and the plates are driven only by the boundary condition, which define the normal component of the outflow from the domain under study, see below. At the top boundary the temperature is set to 0 °C while at the bottom either the temperature $\Delta T = 1200$ °C or zero heat flux is applied. At the left and right sides the temperature is prescribed in order to satisfy the vertical temperature gradient 12 °C per 1 km.

For the Stokes equation, the free-slip boundary condition:

$$\boldsymbol{v} \cdot \boldsymbol{n} = v_0, \tag{5}$$

$$\boldsymbol{D} \cdot \boldsymbol{n} - (\boldsymbol{n} \cdot \boldsymbol{D} \cdot \boldsymbol{n})\boldsymbol{n} = 0, \tag{6}$$

is applied on the top and the bottom of the model. The parameter $v_0 = 0$, except that part of the bottom boundary Γ, where the non-zero outflow v_0 is prescribed. On the left and the right sides, the no-force condition

$$\boldsymbol{D} \cdot \boldsymbol{n} = 0, \tag{7}$$

is used. This set of boundary conditions means that the physical source of motion is the slab pull on Γ. Moreover, neither push nor pull is assumed sufficiently far from the subduction zone.

It has been commonly believed that all rheological properties of the lithosphere should be strongly influenced by the water content (Jung and Karato, 2001). Recent study on the dihedral angles of aqueous fluid in some materials (Ono et al., 2002) has showed that water released from the hydrous mineral can be transported into the deeper mantle. That is why we do not consider any percolation of water from the subducted crust into the overlaying mantle wedge in our shallow model.

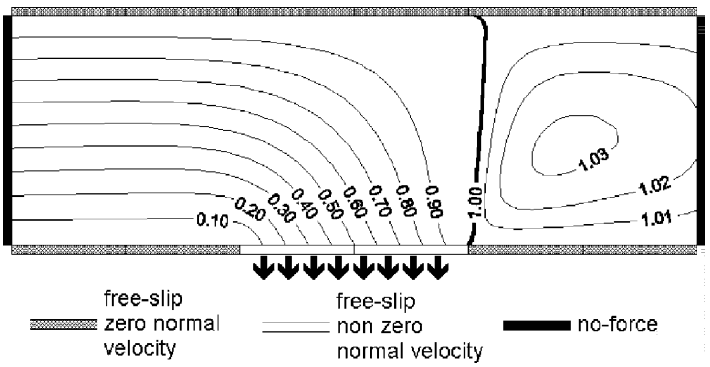

Fig. 1. Scheme of the domain 300×100 km shows where different types of boundary conditions are used. Streamlines for the constant viscosity case scaled by value ψ_s demonstrates the pattern of the flow where no plate-like behaviour is developed.

The key point of our modeling consist in employing the stream function to recognize different parts of the lithosphere. This is possible because in any steady-state case the fluid enclosed by two streamlines cannot be penetrated by the ambient fluid and thus the streamlines separate different parts of the fluid. In other words, chemically different non-reacting material flow along the streamlines without mixing. To avoid extremely high viscosities at low temperatures and to be able to incorporate easily the water content into our model, we replace the rheological relationship (4) by viscosity of the Arrhenius type through the equation:

$$\eta = \eta_{\max} f(\psi) \exp\left(-\frac{\ln(K_t)T}{\Delta T}\right). \tag{8}$$

Here K_t is a parameter controlling the scope of the temperature dependence of viscosity in our models. The zone of weakness due to different chemical composition is imposed by the function $f(\psi)$. The boundary of the incoming (subducting) fluid can now be identified with a streamline $\psi = \psi_s$. Introducing the piece-wise constant function

$$f(\psi) = \begin{cases} w, & \psi \in \langle \psi_s - \delta, \psi_s \rangle, \quad 0 < w < 1 \\ 1, & \text{elsewhere} \end{cases} \tag{9}$$

the zone of weakness can by imposed by parameter w, which yields the reference viscosity $\eta_w = w\eta_0$ in the weakening zone, and also the parameter δ, which affects the thickness of the zone. Although the thickness of the zone of weakness is set by parameter δ, its geometry is not determined a priori and thus the shape of the subducted plate is the output from the modeling.

4. Numerical method

The set of Eqs. (1)–(3) is solved using the finite element method, which is based on the weak formulation. The Eqs. (1) and (2) are fulfilled when the integral equation:

$$\int_\Omega \eta(\nabla \boldsymbol{v} + (\nabla \boldsymbol{v})^T) : \nabla \boldsymbol{u} \, \mathrm{d}\Omega = \int_\Omega \boldsymbol{f} \cdot \boldsymbol{u} \, \mathrm{d}\Omega, \tag{10}$$

holds in a domain under study Ω for each trial vector function $\boldsymbol{u}$, where the solution $\boldsymbol{v}$ is sought from the set of divergence-free functions satisfying all Dirichlet boundary conditions (5) (i.e. the normal components of velocity on the top and the bottom of the domain) considered in the problem and the trial functions $\boldsymbol{u}$ are from the set of divergence-free functions with zero values in the corresponding Dirichlet conditions (Matyska, 1996). On the left-hand side of this equation there is a bilinear form $B(\boldsymbol{v}, \boldsymbol{u})$ that can be written in a symmetric form

$$B(\boldsymbol{v}, \boldsymbol{u}) = 2 \int_\Omega \eta \dot{\boldsymbol{e}}(\boldsymbol{v}) : \dot{\boldsymbol{e}}(\boldsymbol{u}) \, \mathrm{d}\Omega. \tag{11}$$

This formulation incorporates naturally the Neumann boundary conditions (6) and (7) (e.g. Matyska, 1996).

Since we are dealing with a two-dimensional (2D) model, we can use the stream function ψ defined by

$$v_1 = \frac{\partial \psi}{\partial x_2}, \quad v_2 = -\frac{\partial \psi}{\partial x_1}, \tag{12}$$

to satisfy the continuity Eq. (1) identically. According to its definition the stream function is not unique. However, we can easily achieve uniqueness of ψ and satisfy Dirichlet boundary conditions (5) as follows: at the top of the rectangle the stream function is set to a constant value ψ_s. The stream function on the left part of the bottom is set to 0, on the right part it is set to the value ψ_s and in the middle, which is the outflow part of the boundary Γ (see Fig. 1), there is a linear increase from 0 to ψ_s. The value ψ_s is related to the outflow by the formula:

$$\psi_s = \int_\Gamma \boldsymbol{v_0} \cdot \boldsymbol{n} \, \mathrm{d}\Gamma.$$

The bilinear form (11) can be rewritten by means of the stream function:

$$B(\psi, \xi) = \int_\Omega \eta \left(\frac{\partial^2 \psi}{\partial x_1^2} - \frac{\partial^2 \psi}{\partial x_2^2}\right)\left(\frac{\partial^2 \xi}{\partial x_1^2} - \frac{\partial^2 \xi}{\partial x_2^2}\right) \mathrm{d}\Omega + 4 \int_\Omega \eta \frac{\partial^2 \psi}{\partial x_1 \partial x_2} \frac{\partial^2 \xi}{\partial x_1 \partial x_2} \mathrm{d}\Omega.$$

In our models $\Omega = \langle 0, a \rangle \times \langle 0, b \rangle$ is a rectangle, and thus it can easily be divided into rectangular elements through the nodal points

$$x_1^0 = 0, x_1^1 = h_1^1, x_1^2 = h_1^2, \ldots, x_1^{n-1} = a - h_1^n, x_1^n = a,$$
$$x_2^0 = 0, x_2^1 = h_2^1, x_2^2 = h_2^2, \ldots, x_2^{m-1} = b - h_2^m, x_2^m = b,$$

and the basis function ξ^{ij} is the cartesian product $\xi^{ij}(x_1, x_2) = \phi^i(x_1)\phi^j(x_2)$, where the cubic elementary basis functions $\phi^k(x_s)$, $s = 1, 2$, are uniquely determined by the relations

$$\phi^{2k-1}(x_s^l) = \delta_{kl}, \quad \frac{\mathrm{d}\phi^{2k-1}}{\mathrm{d}x}(x_s^l) = 0, \quad \phi^{2k}(x_s^l) = 0, \quad \frac{\mathrm{d}\phi^{2k}}{\mathrm{d}x}(x_s^l) = \delta_{kl}, \tag{13}$$

where δ_{kl} is the Cronecker δ-symbol, see also Křížek and Neittaanmäki (1990). These cubic Hermit elements are used to discretize the stream function and the trial functions.

Similarly, the heat transfer Eq. (3) should be rewritten into its weak formulation

$$\int_\Omega k\nabla T \cdot \nabla\tau \,\mathrm{d}\Omega + \int_\Omega \rho c_p \boldsymbol{v} \cdot \nabla T\tau \,\mathrm{d}\Omega = \int_\Omega \boldsymbol{D} : \nabla \boldsymbol{v}\tau \,\mathrm{d}\Omega, \tag{14}$$

for all trial scalar functions τ, which are zero on such a part Γ of the boundary, where temperature T is prescribed. Such a formulation includes zero heat flux boundary condition on the rest of the boundary $\partial\Omega \setminus \Gamma$. The basis function τ^{ij} is the cartesian product $\tau^{ij} = \theta^i(x_1)\theta^j(x_2)$, where the elementary basis function $\theta^k(x_s)$ are chosen to be piece-wise linear and uniquely determined by the relation

$$\theta^k(x_s^l) = \delta_{kl}. \tag{15}$$

The set of Eqs. (1)–(3) is strongly non-linear for a temperature dependent viscosity, but it can be readily solved using a simple iterative procedure, which utilizes the fact, that for a fixed temperature field (i.e. given viscosity distribution) the Stokes Eq. (2) is linear in $\boldsymbol{v}$ and also the heat transfer equation is linear in T for a fixed velocity field. This leads to an iterative scheme as follows

$$T^0 \Rightarrow \psi^0 \Rightarrow T^1 \Rightarrow \psi^1 \Rightarrow \cdots \Rightarrow T^n \Rightarrow \psi^n \Rightarrow T^{n+1} \Rightarrow \psi^{n+1} \Rightarrow \cdots, \tag{16}$$

which converges quite well when the modified temperature $\hat{T}^n$ given by

$$\hat{T}^n = \alpha T^n + (1-\alpha)T^{n-1}, \tag{17}$$

where T^n is the solution of nth iteration of the heat transfer equation and α is the damping parameter $0 < \alpha < 1$, is used in the nth iteration of the Stokes equation instead of T^n. In this study we take into account the stream function dependence of viscosity. In order to improve the rate of convergence, the modified stream function

$$\hat{\psi}^n = \beta\psi^n + (1-\beta)\psi^{n-1}, \tag{18}$$

should be used in the iterative process instead of ψ^n. Similarly as in the Eq. (17), β is the damping parameter here, $0 < \beta < 1$. Optimal values of parameters α and β differ from case to case, but a value between 0.1 and 0.2 yields sufficient results in most cases of this study.

5. Results of parameter studies

All studied cases were computed using a new code written in Fortran 90. The code was successfully tested on benchmarks used in geophysics (Blankenbach et al., 1989), which differs from standard benchmarks (de Vahl David and Jones, 1983) by neglecting inertial forces.

As already demonstrated in Fig. 1, lack of the zone of weakness results into a flow without a plate-like behavior and thus its presence in our modeling is necessary. In all studied cases the zone of viscosity weakening was determined by setting $\delta = 0.1\psi_s$, which means that zone of weakness was approximately 10 km thick corresponding thus to the oceanic crust. Slightly thicker oceanic crust was applied to use sparse mesh and save CPU time.

Since we set $\eta_{\max} = 10^{24}$ Pa s, the magnitude of K_t was set to 10^3 in most of the studied cases to obtain commonly accepted value of the viscosity at the bottom of the lithosphere. The first set of numerical experiments (Fig. 2) was performed for a very slow plate (plate velocity $v_0 = 1$ cm per year). The viscosity drop w in the zone of weakness strongly affects the pattern of the flow and the dip angle of the subducted plate. One can clearly recognize that for the chosen values of w the dip angle changes from 90° to approximately 45°. On the other hand, the temperature field was not strongly affected by these viscosity changes. We have also tested the influence of dissipation by neglecting the rhs of (14). The maximal change of temperature was less than tens of degrees in all studied cases of viscosity drops, which means

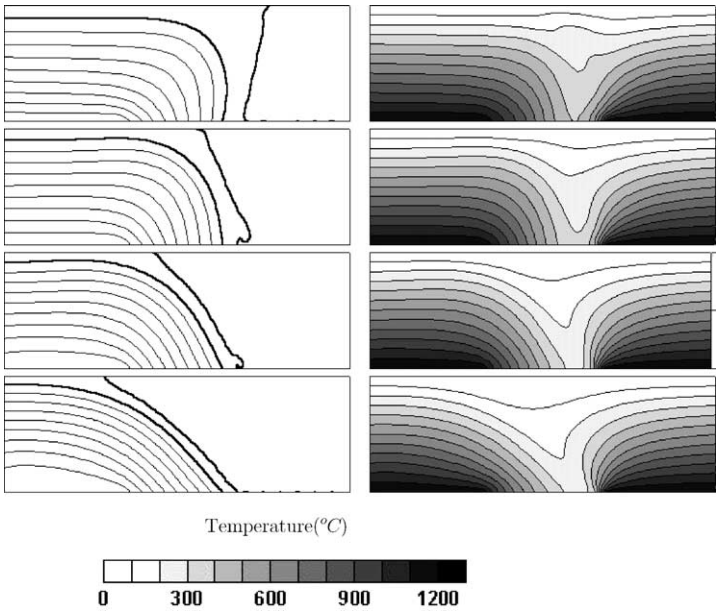

Fig. 2. Temperature (right) and streamlines (left) in the case of plate velocity $v_0 = 1$ cm per year with dissipation. Reference viscosity $\eta_0 = 10^{24}$ Pa s, the weakening parameter w changes from top to bottom: $10^{-1}, 10^{-2}, 10^{-3}$ and 10^{-4}. Streamlines bounding the zone of weakness are marked by thick lines. Parameter K_t is set to 10^3.

that the dissipative heating need not be taken into account for slow subductions.

If the plate velocity is higher, dissipation plays a substantial role, see Figs. 3 and 4, where $v_0 = 5$ cm per year was chosen. Although dissipation is included in Fig. 3 and neglected in Fig. 4, there are not substantial differences in velocities for corresponding viscosity drops. The changes of the dip angle are similar

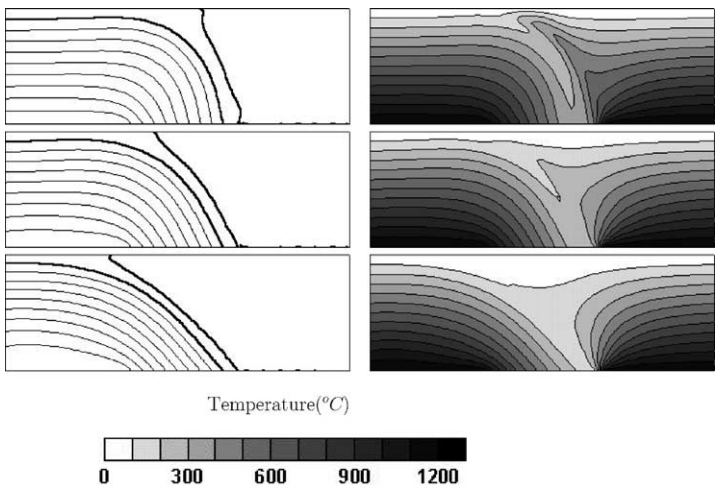

Fig. 3. Temperature (right) and streamlines (left) in the case of plate velocity $v_0 = 5$ cm per year with dissipation. Reference viscosity $\eta_0 = 10^{24}$ Pa s, the weakening parameter w changes from top to bottom: $10^{-2}, 10^{-3}$ and 10^{-4}. Streamlines bounding the zone of weakness are marked. Parameter K_t is set to 10^3.

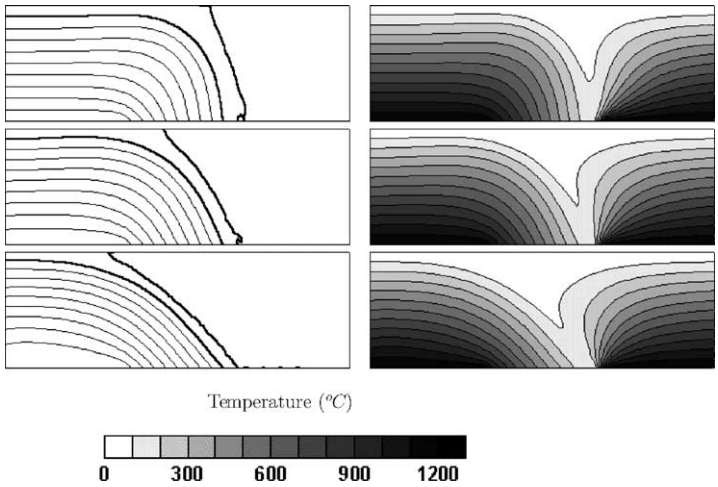

Fig. 4. Same as Fig. 3, but dissipation is not included.

to those for a slow subduction. However, dissipative heating produces remarkable increases of temperature mainly at the contact zone. The maximal change of temperature obtained by excluding the dissipation was several hundreds of degrees; therefore realistic thermal models of subductions should incorporate this effect. The viscosity drop is a key parameter influencing temperature increases at the plate contact; the highest

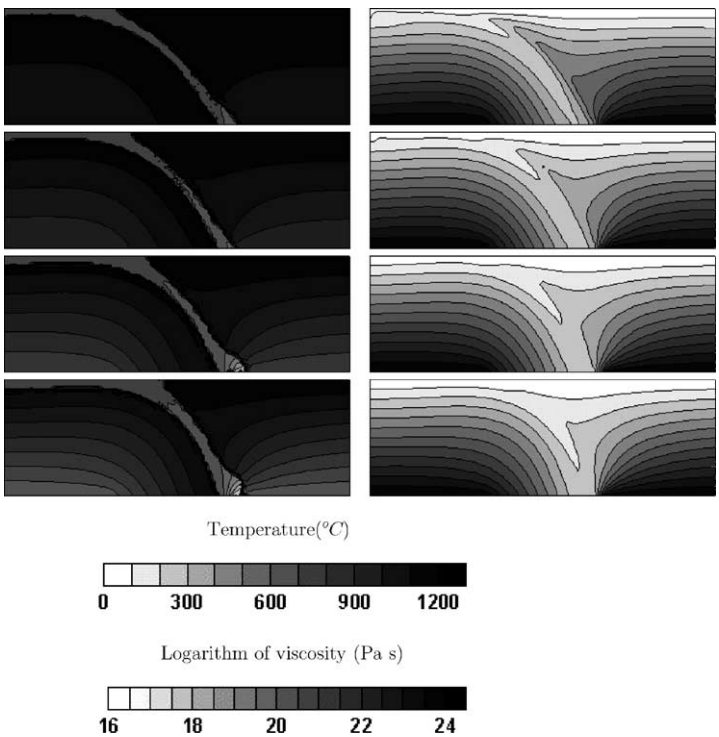

Fig. 5. Temperature (right) and logarithm of viscosity (left) in the case of plate velocity $v_0 = 5\,\mathrm{cm}$ per year with dissipation. Reference viscosity $\eta_0 = 10^{24}\,\mathrm{Pa\,s}$, the weakening parameter $w = 10^{-3}$. Parameter K_t changes from top to bottom: 10^1, 10^2, 10^3 and 10^4.

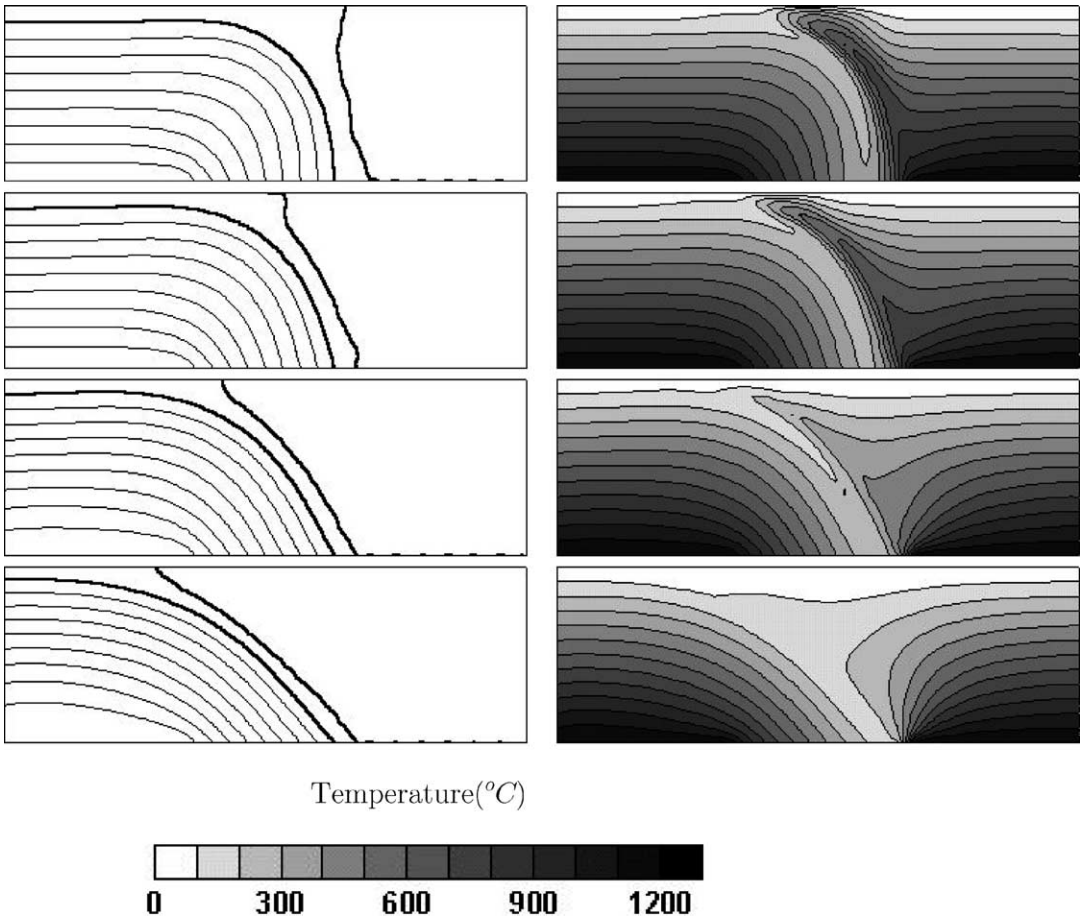

Fig. 6. Temperature (left) and streamlines (right) in the case of plate velocity $v_0 = 10$ cm per year with dissipation. Reference viscosity $\eta_0 = 10^{24}$ Pa s, the weakening parameter w changes from top to bottom: $3 \times 10^{-2}, 10^{-2}, 10^{-3}$ and 10^{-4}. Streamlines bounding the zone of weakness are marked by thick lines. Parameter K_t is set to 10^3.

temperature changes are obtained when viscosity drop is relatively small.

When the parameter K_t, which controls the sensitivity of viscosity on temperature according to (8), is changed, the subduction dip changes are relatively small. Fig. 5 shows results of numerical experiments where parameter K_t has been changed in a wide range between 10 and 10^4. The changes in subduction dip were less than 15 degrees. Although changes of velocity field were relatively small, the temperature field was much more sensitive to the magnitude of K_t as higher values of K_t result in stronger viscosity decrease in the zone of weakness (and, of course, also in the ambient plates), which suppresses dissipation. Temperature dependence of viscosity is thus a feedback mechanism, which controls possible increases of temperature at the contact between the plates.

Dissipative heat becomes more stronger with increasing plate velocity, which is shown in the case $v_0 = 10$ cm per year (Fig. 6). For small viscosity drop ($w = 0.1$) in the zone of weakness the plate contact becomes unrealistically overheated. Although differences in the velocity field are higher in comparison with smaller v_0, the main feature still remains: to create straight and narrow slip zone between subducting and overriding plates, viscosity drop of several orders is needed. If the viscosity drop is not sufficient (one order or less) either plate-like behavior is not observed

or the plate sinks into the deeper mantle nearly vertically. Here, should be pointed out that in the cases of low reference viscosity in the weakening zone η_w, the stream function scaled by value ψ_s for plate velocity between 1 and 10 cm per year is nearly the same, which implies that dissipative heat does not play important role in such cases.

6. Conclusion

This paper presents new possibility how to incorporate the zone of weakness into the modeling of subducting plates. Such a zone can be imposed using the viscosity law, which depends on the stream function. This approach is suitable for self-consistent inclusion of a change in chemical composition of subducting lithosphere, e.g. due to the content of water. The main advantage of this formulation is that there is no a priori assumption about the shape of bending lithosphere. This means that also the dip angle of the subducting plate is obtained a posteriori.

Influence of dissipative heating has been investigated in some numerical models (e.g. Ponko and Peacock, 1995; Currie et al., 2002). In these models the shear heating is prescribed only at the fault or in a narrow surrounding zone and the increase in the temperature due to shear heating is up to 200 °C. In our model, where the shear heating is computed in the whole box, its effect on geometry of the slab is small, but temperature field for fast subduction can be influenced more than in cited studies and therefore dissipative heating should not be neglected. Because of temperature dependence of phase changes, dissipation can play an important role in mineralogical consideration concerning the state of subducting plates.

Significant results of this kind of modeling show that viscosity weakening of the uppermost part of the lithosphere can produce narrow slip contact zone between plates and moreover the dip of subducted plates strongly depends on the magnitude of the weakening, which may be affected by the chemical composition of the crust, mainly by the water content. It was shown that a purely non-linear viscous model can produce slab dips in the observed range (Jarrard, 1986). Results of our numerical models also lead to the hypothesis that plates with higher water content in the oceanic crust sink into the mantle with shallower dips. Viscosity decrease of several orders of magnitude in the zone of weakness is necessary in order to prevent overheating at the contact.

Although many complicated rheology types including some weakening mechanism (stress yielding, Peierls creep, grain size, etc.) are used in current models of subducting plates, the plate-like behavior of the lithospheric plates can be simply the result of different chemical composition of the crust and the remaining part of the lithosphere.

Acknowledgements

This research was supported by the Research Project DG MSM 113200004 and Charles University Grant 238/2001/B-GEO/MFF. M. Kukačka was partly supported by the Czech national grant No. 205/02/1306 and C. Matyska by the Czech national grant No. 205/03/0778. M.-P. Doin and an anonymous reviewer are gratefully acknowledged for their constructive comments.

References

Bercovici, D., 1995. A source-sink model of the generation of plate tectonics from non-Newtonian mantle flow. J. Geophys. Res. 100, 2013–2030.

Bercovici, D., 1996. Plate generation in a simple model of lithosphere-mantle flow with dynamic self-lubrication. Earth Planet. Sci. Lett. 144, 41–51.

Bercovici, D., 2003. The generation of plate tectonics from mantle convection. Earth Planet. Sci. Lett. 205, 107–121.

Billen, M.I., Gurnis, M., 2001. A low viscosity wedge in subduction zones. Earth Planet. Sci. Lett. 193, 227–234.

Bina, C.R., Stein, S., Marton, F.C., van Ark, E.M., 2001. Implications of slab mineralogy for subduction dynamics. Phys. Earth Planet. Inter. 127, 51–66.

Bird, P., 1978. Finite elements modeling of lithosphere deformation: the Zargos collision orogeny. Tectonophysics 50, 307–336.

Blankenbach, B., et al., 1989. A benchmark comparison for mantle convection codes. Geophys. J. Int. 98, 23–38.

Currie, C.A., Hyndman, R.D., Wang, K., Kostoglodov, V., 2002. Thermal models of the Mexico subduction zone: implication for the megathrust seismogenic zone. J. Geophys. Res. 107 (art. no. 2370).

Čížková, H., van Hunen, J., van den Berg, A.P., Vlaar, N.J., 2002. The influence of rheological weakening and yield stress on the interaction of slabs with the 670 km discontinuity. Earth. Planet. Sci. Lett. 199, 447–457.

de Vahl Davis, G., Jones, I.P., 1983. Natural convection in a square cavity: a comparison exercise. Int. J. Num. Methods Fluids 3, 227–248.

Doin, M.-P., Henry, P., 2001. Subduction initiation and continental crust recycling: the roles of rheology and eclogitization. Tectonophysics 342, 163–191.

Jarrard, R.D., 1986. Relations among subduction parameters. Rev. Geophys. 24, 217–286.

Jung, H., Karato, S.I., 2001. Effect of water on dynamically recli-stallized grain-size of olivine. J. Struct. Geol. 23, 1337–1344.

Karato, S.I., in press. Mapping water content in the upper mantle. In: Eiler, J. (Ed.), Subduction Factory. AGU Monograph, in press.

Karato, S.I., Wu, P., 1993. Rheology of the upper mantle: a synthesis. Science 260, 771–778.

Kohlstedt, D.L., Evans, B., Mackwell, S.J., 1995. Strength of the lithosphere: constraints imposed by laboratory experiments. J. Geophys. Res. 100, 17587–17602.

Křížek, M., Neittaanmäki, P., 1990. Finite Element Approximation of Variational Problems and Application. Longman, New York.

Lenardic, A., Kaula, W.M., 1994. Self-lubricated mantle convection: two-dimensional models. Geophys. Res. Lett. 21, 1707–1710.

Lithgow-Bertelloni, C., Richards, M.A., 1998. The dynamics of Cenozoic and Mesozoic plate motions. Rev. Geophys. 36, 27–78.

Matyska, C., 1996. Variational principles for the momentum equation of mantle convection with Newtonian and power-law rheologies. Geophys. J. Int. 126, 281–286.

Ono, S., Miebe, K., Yoshino, T., 2002. Aqueous fliud connectivity in pyrope aggregates: water transport into the deep mantle by a subducted oceanic crust without any hydrous minerals. Earth. Planet. Sci. Lett. 203, 895–903.

Peacock, S., 2000. Thermal and petrologic structure of subduction zones. In: Bebout, G.E., Scholl, D.W., Kirby, S.H., Platt, J.P. (Eds.), Subduction: Top to Bottom. AGU Monograph 96, pp. 119–133.

Ponko, S.C., Peacock, S.M., 1995. Thermal modeling of the southern Alaska subduction zone: insight into the petrology of the subducting slab and overlying mantle wedge. J. Geophys. Res. 100, 22117–22128.

Regenauer-Lieb, K., Yuen, D.A. Modeling shear zones in geological and planetary sciences: solid- and fluid thermal-mechanical approaches. Earth Sci. Rev., submitted for publication.

Ribe, N.M., 1992. The dynamics of thin shells with variable viscosity and the origin of toroidal flow in the mantle. Geophys. J. Int. 110, 537–552.

Tackley, P.J., 2000. Self-consistent generation of tectonic plates in time-dependent, three-dimensional mantle convection simulations: 1. Pseudoplastic yielding. G^3, 1: Paper number 2000GC000036.

Tackley, P.J., 2000. Self-consistent generation of tectonic plates in time-dependent, three-dimensional mantle convection simulations: 2. Strain weakening and asthenosphere. G^3, 1: Paper number 2000GC000043.

van Hunen J., 2001. Shallow and Buoyant Lithospheric Subduction: Causes and Implications from Thermo-chemical Numerical Modeling. Ph.D. Thesis, Geologica Ultraiectina No. 211, Utrecht University.

Vilotte, J.P., Daigni, M., Madariaga, R., 1982. Numerical modelling of intraplate deformation: simple mechanical models of continental collision. J. Geophys. Res. 87, 10709–10728.

Watts, A.B., 2001. Isostasy and Flexture of the Lithosphere. Cambridge University Press, Cambridge.